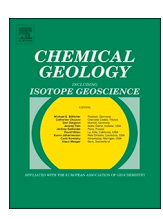


Contents lists available at ScienceDirect

Chemical Geology

journal homepage: www.elsevier.com/locate/chemgeo



Lithium isotope compositions of U.S. coals and source rocks: Potential tracer of hydrocarbons



Zebadiah Teichert*, Maitrayee Bose, Lynda B. Williams

School of Earth and Space Exploration, Arizona State University, Tempe, AZ 85287-1404, United States of America

ARTICLE INFO

Editor: Oleg Pokrovsky

Keywords:
Lithium isotopes

Kerogen
Coal

Hydrocarbon source rocks
Secondary Ion Mass Spectrometry (SIMS)
NanoSIMS

ABSTRACT

Kerogen in organic-rich rocks contains trace amounts of lithium (Li) that has been overlooked as a contributor to the global Li geochemical cycle. This study examined a variety of coals where kerogen is concentrated (> 50% organic carbon) and hydrocarbon source rocks of different ages, depositional environments and thermal maturity to determine their range of Li isotopic compositions (8^7 Li‰) and factors that influence their compositions.

Using Secondary Ion Mass Spectrometry (SIMS), we analyzed 22 coals and 4 hydrocarbon source rocks (Types I, II, III), to determine the $\delta^7 \text{Li}$ of kerogen in situ, without chemical isolation of phases that can alter their original isotopic compositions. The $\delta^7 \text{Li}$ values of the coals surveyed are distinctly isotopically light (< 0‰) compared to most natural minerals and fluids. In immature coals, with a vitrinite reflectance in oil (VRo) of \leq 0.5%, kerogen $\delta^7 \text{Li}$ values average $-23.4 \pm 1.1\%$ and become heavier with increasing thermal grade to temperatures of gas generation (VRo \sim 1.3%). The linear correlation between $\delta^7 \text{Li}$ and VRo suggests that $^6 \text{Li}$ may be preferentially released to pore fluid from kerogen during thermal maturation. Notably, authigenic clays forming at diagenetic temperatures substitute Li from pore fluids into silicate layers, therefore, the Li isotopic composition of the clays may record fluid isotopic compositions influenced by organic-Li sources.

NanoSIMS isotopic maps of the Lower Bakken Shale, and SIMS measurements of the Green River Shale show isotopically light Li associated with C-dominated areas, and heavier δ^7 Li with Si-dominated areas of the hydrocarbon source rocks. We conclude that kerogen is a source of isotopically light Li that contributes to fluids during thermal maturation and hydrocarbon generation. Kerogen may be a significant contributor of Li to pore fluids and its distinctly light Li isotopic composition relative to other terrestrial waters and minerals could provide a tracer of organic inputs to the global geochemical cycle.

1. Introduction

Lithium isotopes are being increasingly utilized to aid in understanding a host of terrestrial and extraterrestrial processes. In terrestrial systems, there has been significant use of Li isotopes in low temperature crustal environments to investigate the geologic processes of weathering and fluid dynamics (Penniston-Dorland et al., 2017; Tomascak et al., 2016). However, there is limited information regarding how Li from organic compounds may play a role in these processes. If there is a significant amount of Li bound in organic compounds, it is important to know its isotopic composition and how Li from organics would contribute to the global geochemical cycle if the Li were released from the organics (e.g. with increasing burial temperature). In this study, we measured the Li isotope compositions on a suite of 22 coals from across the United States, representing different ages, depositional environments and thermal maturities. In addition, 4 hydrocarbon source rocks

containing Type I, II and/or III kerogen were analyzed using Secondary Ion Mass Spectrometry (SIMS) and NanoSIMS. The goal of this study is to evaluate the range of Li isotopic compositions in organic-rich rocks consisting of a variety of organic macerals which were exposed to a range of thermal alteration conditions.

1.1. Lithium resources

Lithium is an important natural resource that has increased in demand due to the rising use of Li ion batteries. The primary economic sources for Li are brines, salt lakes and pegmatite deposits (Kesler et al., 2012). Seawater contains only ~ 0.17 mg/L Li but it is extracted economically using manganese oxide membranes to concentrate Li (Hong et al., 2018). Lithium is more concentrated in oilfield brines with concentrations up to several 100 mg/L (Collins, 1975; Eccles and Berhane, 2011; Macpherson, 2015; Millot et al., 2011; Phan et al.,

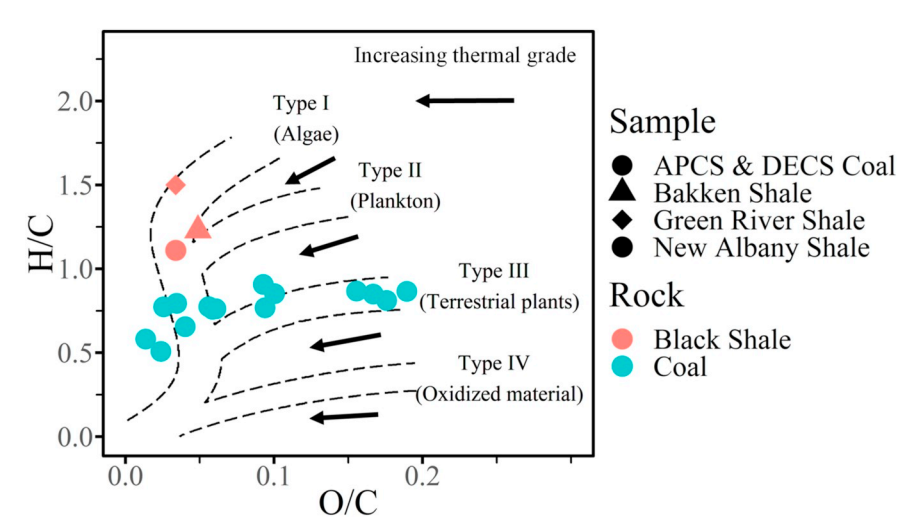
^{*} Corresponding author at: Physical Sciences F-686, 550 E. Tyler Mall, Arizona State University, Tempe, AZ, United States of America. E-mail address: zteicher@asu.edu (Z. Teichert).

2016). Interestingly, Li concentrations in bitumen (extractable organic compounds) are reported to be higher than their reservoir rocks by up to 17 mg/L, suggesting an association of Li with extractable hydrocarbons (Hosterman, 1990). In hydrocarbon source rocks, Li concentrations are highest in authigenic clay minerals (primarily illitesmectite; I-S) and some studies suggest that Li may be linked to gas generation (Williams et al., 2013, 2015). Lithium substitutes in the octahedral sites of I-S and is also adsorbed in clay interlayers (Sposito et al., 1999). Bentonite from hydrocarbon reservoirs in the Baltic Basin, contain I-S with Li contents > 600ppm after removal of interlayer-Li (Williams et al., 2013), whereas average marine shales have a reported range of 50-75 ppm Li (Horstman, 1957; Pendias and Kabata-Pendias, 2000). In Marcellus Shale source rock, Phan et al. (2016) found organics and sulfide minerals to be the second largest (up to 20%) host for Li after the silicate fraction. For coals, the worldwide average reported Li-content is lower than for clays, with ranges from 6 to 44 ppm (Finkelman et al., 2018; Ketris and Yudovich, 2009; Swanson, 1975). However, some coals from China have been identified as containing economically viable concentrations of Li (Qin et al., 2015). Coals within the Jungar Coalfield (Mongolia) have Li concentrations exceeding 500 ppm but in those deposits, Li is mostly concentrated in authigenic clays within the coal (Dai et al., 2012).

1.2. Geologic background

Kerogen is the insoluble organic material found in sedimentary rocks (Durand, 1980) that is derived from the remains of organisms and is the most abundant form of organic matter on Earth (Vandenbroucke and Largeau, 2007). Kerogen is composed of a variety of organic macerals, which are grouped based on their physical properties. Just as rocks are composed of multiple minerals that each might host Li, the macerals that comprise kerogen may each host Li in different structural arrangements. Because of the complexity of organic macerals in kerogen, a simple approach to assessing major compositional changes was developed by Van Krevelen (1950) comparing their major element ratios (H/C and O/C) to classify organic Types (e.g., I, II, III) (Fig. 1).

Coals contain primarily Type III kerogen derived from woody remains of plants that contain high O/C and low H/C (Vandenbroucke and Largeau, 2007). Coals are dominated by vitrinite (> 70% by volume; Orem and Finkelman, 2003), which is a group of organic macerals that can indicate the thermal maturity according to its reflectance in oil immersion microscopy (VRo; Mukhopadhyay, 1994). Type III kerogen is more prone to generate gas than liquid hydrocarbons. Types I and II kerogen are primarily derived from algae and phytoplankton, containing higher H/C and lower O/C and are more prone to generate liquid hydrocarbons (Vandenbroucke and Largeau, 2007).



1.3. Lithium isotope measurements of kerogen

Lithium is a valuable tracer of fluids because of its mobility during surface weathering and under hydrothermal conditions (Millot et al., 2010; Pistiner and Henderson, 2003). Lithium isotopes are commonly used for tracing lithologic sources that contribute Li to fluids (e.g., Misra and Froelich, 2012; Williams et al., 2013, 2015; Phan et al., 2016), as different sources have a range of Li isotope ratios (Fig. 2).

In this study, we measured Li isotopic compositions in kerogen using solid-state secondary ion mass spectrometry (SIMS), because it has been recognized that reagents (acids) used to isolate kerogen (or insoluble organic matter (IOM); Cronin et al., 1987) from sediments also react with organic functional groups in kerogen, thus altering their composition (Saxby, 1976). To demonstrate this, Williams and Bose (2018) extracted kerogen from the Lower Bakken shale using standard 5 N HF- 1 N HCl digestion (Durand, 1980) and compared the ⁷Li/¹²C ratio of the acid treated IOM ($^{7}\text{Li}/^{12}\text{C} = 0.024 \pm 0.004$; n = 5) to unextracted kerogen in polished section ($^{7}\text{Li}/^{12}\text{C} = 0.244 \pm 0.020$; n=6). This indicates an average loss of 90% Li from the acid treated kerogen. Furthermore, NanoSIMS in situ measurements were made (using a 300 nm spot size) of ⁷Li/¹²C on kerogen in an argon ion polished section of the same Bakken sample. This sample preparation makes it easier to avoid beam overlap with silicates, and the average 7 Li/ 12 C ratio on kerogen was even higher (0.414 \pm 0.020; n = 11) confirming significant loss of organolithium in the acid treated IOM. To our knowledge, this study is the first survey of Li isotopes in kerogen that has not been isolated from silicates by acid treatments, which likely alters their Li isotopic ratios.

2. Methods

2.1. Samples

Powdered coal samples (< 0.25 mm) were obtained from the Pennsylvania State University (PSU) coal repository and the National Institute of Standards and Technology (NIST). The PSU samples included 8 Department of Energy Coal Samples (DECS) and 7 Argonne National Laboratory Premium Coal Samples (APCS). Additionally, 3 NIST coal samples, 4 coal samples from mines in the Rocky Mountain region of the U.S., and 4 hydrocarbon source rocks were acquired to extend the range of age, thermal grade and kerogen Types studied. The coal samples come from most of the major sedimentary basins in the U.S., range in VRo from 0.25–5.19%, and in age from the Carboniferous to the Tertiary. Table 1 lists the samples studied and source rock data are shown in Table 2.

Additional bulk coal samples were studied in thick polished sections

Fig. 1. Van Krevelen plot (Van Krevelen, 1950; modified by McCarthy et al., 2011) of coal and source rock samples studied. For Bakken Shale and New Albany Shale O/C values were approximated from Oxygen Index values (Akar, 2014; Jin, 2014; Jones, 1981; Lewan and Ruble, 2002; Peters et al., 2016). This van Krevelen diagram shows the range of kerogen Types studied in this work.

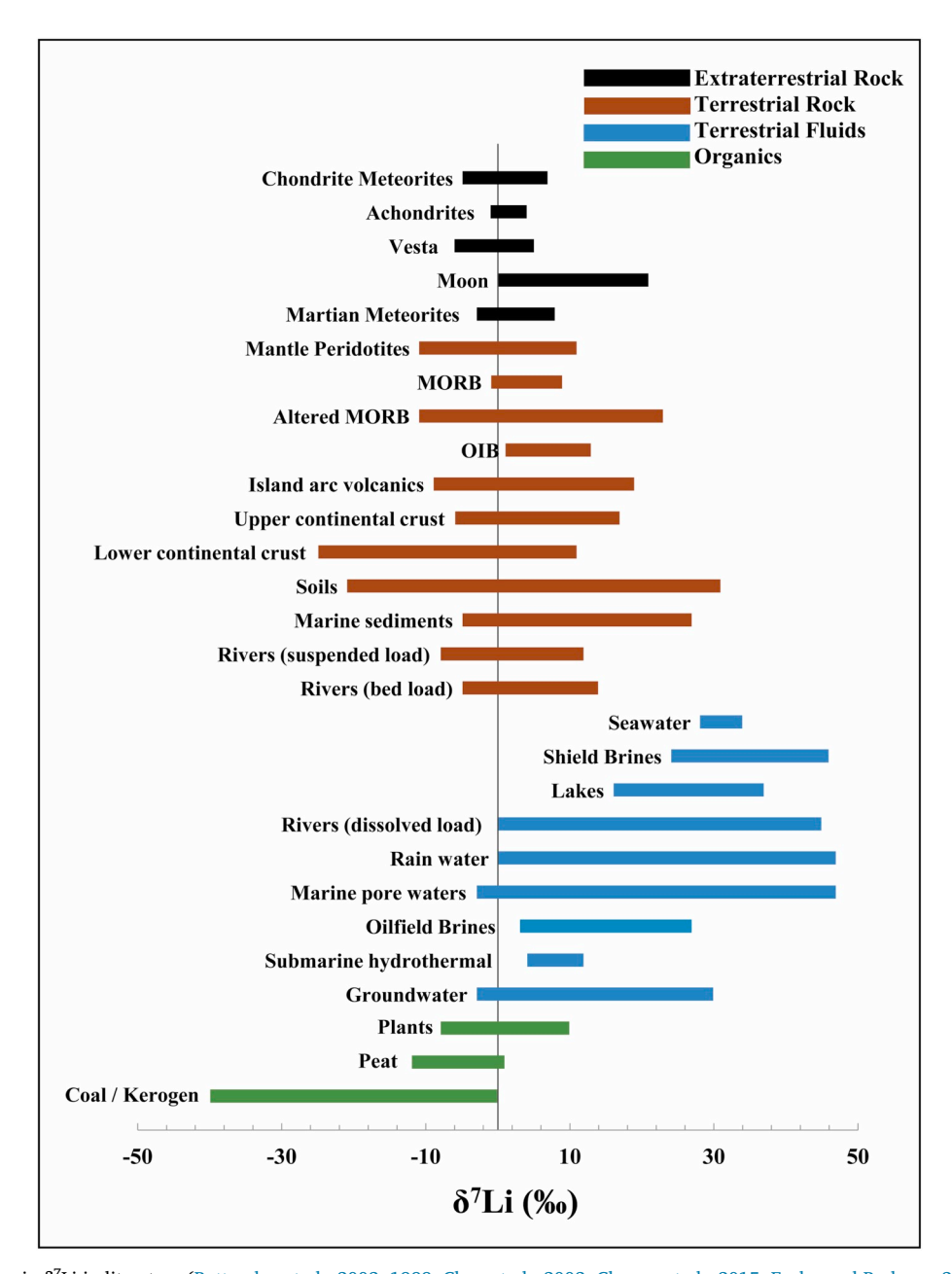


Fig. 2. Natural variations in δ^7 Li in literature (Bottomley et al., 2003, 1999; Chan et al., 2002; Clergue et al., 2015; Eccles and Berhane, 2011.; Lemarchand et al., 2010; Macpherson et al., 2014; Millot et al., 2011; Négrel et al., 2010; Penniston-Dorland et al., 2017; Phan et al., 2016; Tomascak et al., 2016). Coal/kerogen measurements are from this study and contain lower δ 7Li values than all other Li-reservoirs.

for comparison to the powdered samples. These samples came from the Williston Basin (Montana), Powder River Basin (Wyoming) and San Juan River Basin (New Mexico). Two of the whole rock samples are from the Fruitland Fm. of the San Juan River Basin and were selected specifically because of their high (up to 39 ppm) Li content (Bregg et al., 1998), relative to average sub-bituminous coals (6–7 ppm). Coal from the Powder River Basin was selected because of its low ash content, while the coal from Williston Basin was obtained to determine the reproducibility of Li isotope compositions of samples taken from separate locations within the same deposit (DECS-25 and the Savage Lignite).

Source rock shales (Table 2) were acquired from the US Geological Survey (Denver, CO) and were previously studied for B isotope compositions (Williams and Hervig, 2004). These rocks were selected to determine whether the Li isotopic composition varied with organic Type; Type I (Green River Fm.), Type II (New Albany Fm.), Type I/II

(Bakken Fm. Lower Bakken) and Type III (Wilcox Fm.). The Green River Fm. (Type 1) is the type locality for lacustrine deposition (Bradley, 1931). The kerogen found in these deposits comes primarily from algal sources, with total organic carbon (TOC) up to 15.8% (Vandenbroucke and Largeau, 2007). The Type II New Albany Fm. Blocher member from the Eastern Interior Basin contains TOC up to 9.4% (Lewan et al., 1995) and represents a typical Type II kerogen marine shale, where planktonic organisms are the primary input (Vandenbroucke and Largeau, 2007). The Lower Bakken Fm. (Type I/II) from the Williston Basin has a variable TOC up to 35% (Jin and Sonnenberg, 2012) and contains inputs of both terrestrial and planktonic origin where it was deposited in an offshore ramp depositional environment (Albert, 2014). Wilcox Fm. (Type III) from the Gulf of Mexico Sedimentary Basin has a primary input of higher plants and was deposited in a wide range of depositional environments (lagoonal, fluvial, and deltaic) (Nichols and Traverse, 1971). The Wilcox sample we analyzed is a lignite with > 50% TOC.

Table 1
Coal data from the Penn. State Coal Repository and Lithium isotope data from this study.

				Coal data								This study		
Sample	State	Geologic age	Ash dry %	V.M dmmf %	C dmmf %	H dmmf %	O dmmf %	N dmmf %	Vit %	VRo %	Li (ppm) USGS	δ7Li ‰ ± S.E.	Li/C *100	n
Argonne Nation	al Labo	ratory Premium	Coal Sample	s										
1	PA	Carboniferous	13.18	30.1	88.08	4.84	4.72	1.60	71	1.16	15	-5.5 ± 2.7	2.8 ± 0.9	7
2	WY	Tertiary	8.77	48.5	76.04	5.42	16.90	1.13	89	0.32	3.9	-24.0 ± 5.0	0.8 ± 0.1	6
3	IL	Carboniferous	15.48	45.7	80.73	5.20	10.11	1.43	85	0.46	7.7	-25.9 ± 5.3	2.3 ± 0.5	9
4	PA	Carboniferous	9.25	40.8	84.95	5.43	6.90	1.68	85	0.81	8.9	-17.2 ± 4.3	4.2 ± 1.0	4
5	VA	Carboniferous	4.77	19.0	91.81	4.48	1.66	1.34	89	1.68	5.5	-21.9 ± 2.7	1.7 ± 0.6	3
6	UT	Cretaceous	4.71	47.8	81.32	5.81	10.88	1.59	86	0.57	5.5	-16.5 ± 2.1	4.3 ± 0.8	2
7	WV	Carboniferous	19.84	36.2	85.47	5.44	6.68	1.61	73	0.89	27	-14.0 ± 1.4	5.3 ± 1.2	6
8	ND	Tertiary	9.72	49.2	74.05	4.90	19.13	1.17	nr	0.25	2.7	nr	$2.5~\pm~1.0$	
Department of I	Energy (Coal Samples												
1	TX	Tertiary	15.81	55.5	76.13	5.54	15.78	1.50	78	0.36	nr	-15.7 ± 2.4	2.4 ± 0.6	13
3	CO	Cretaceous	5.37	28.2	87.78	5.85	4.03	1.76	94	1.28	nr	-4.6 ± 0.15	0.4 ± 0.1	4
6	UT	Cretaceous	5.84	46.9	81.72	6.22	10.10	1.56	69	0.66	nr	-16.5 ± 2.8	3.3 ± 0.3	4
21	PA	Carboniferous	11.15	3.9	91.87	3.91	2.92	0.81	87	5.19	nr	-39.4 ± 3.9	13.6 ± 1.5	10
22	PA	Carboniferous	23.27	37.8	88.64	5.75	3.03	1.86	30	0.77	nr	-12.5 ± 2.9	4.0 ± 0.6	4
25	MT	Tertiary	11.85	46.9	75.64	5.15	17.72	1.09	74	0.23	nr	-24.3 ± 4.5	1.7 ± 0.8	5
34	PA	Carboniferous	7.35	40.4	85.41	5.55	6.38	1.72	83	0.83	nr	-12.4 ± 6.3	2.3 ± 0.7	3
39	WY	Tertiary	8.03	64.6	74.75	5.43	18.87	1.01	84	0.3	nr	-25.9 ± 3.0	2.3 ± 1.2	5
National Institu	te of Sta	andards and Tec	hnology Sam	ples										
1632c unrinsed	PA	Carboniferous	7.16	nr	77.45	5.11	nr	1.50	nr	0.81	nr	-32.5 ± 7.7	2.0 ± 0.4	2
2682b	WY	Tertiary	6.32	48.5	68.43	4.88	16.24	nr	89	0.32	nr	-42.0 ± 7.0	0.4 ± 0.1	3
2684b	IL	Carboniferous	10.85	36.4	69.25	4.59	nr	1.45	nr	0.75	nr	-12.1 ± 4.6	2.8 ± 1.0	3
Additional coal	sample	s of this study												
San Juan	NM	Cretaceous	16.77	40.05*	69.90*	nr.	nr.	nr.	67.6	0.51	nr	-27.1 ± 5.6	2.0 ± 0.9	7
Four Corners	NM	Cretaceous	15.78	38.12*	70.30*	nr.	nr.	nr.	75.2	0.5	nr	-27.4 ± 0.1	1.9 ± 1.1	33
Savage	MT	Tertiary	4.89	47.26*	71.20*	nr.	nr.	nr.	32.8	0.27	nr	-27.6 ± 2.2	nr	2
Black thunder	WY	Tertiary	4.92	41.90*	72.71*	nr.	nr.	nr.	24.4	0.39	nr	-27.3 ± 1.7	$0.2 ~\pm~ 0.1$	21

Chemical data (wt%) is calculated moisture free; dmmf – Dry mineral matter free; S.E. – 1σ standard errors; nr - not reported; VRo- vitrinite reflectance; VM- volatile material

2.2. Sample preparation

To remove surface adsorbed Li on minerals and organic macerals, all samples were rinsed in 1.82% mannitol solution which was shown to complex with B(OH)₃ (Hingston, 1964; Tonarini et al., 1997) for removal of surface adsorbed B. Mannitol also complexes with surface adsorbed Li(OH) and was shown to significantly reduce Li contents of clay separates (Williams et al., 2015). After sonication and soaking in mannitol 24 h., the samples were rinsed in triplicate using Nanopure water (18.5 M Ω -cm resistivity), centrifuged to settle, and dried at 60 °C. Powdered samples were then pressed into round flat pellets using a Carver die press at 9000 psi for ~5 min. DECS-21 powder, with the highest VRo (5.19%), was too brittle to press into a pellet and was instead pressed into indium for analysis. Source rocks and additional coal samples were made into polished thick sections. Samples were heated to 60 °C overnight to remove surface volatiles for better vacuum in the SIMS instruments. To alleviate sample charging a thin conductive gold

coat (20–50 nm) was applied to sample surfaces using a gold coater (Hummer 6.2 by Anatech Inc.).

2.3. Lithium isotopes

The stable isotopes of Li include ^7Li that makes up 92.58% and ^6Li that makes up 7.42% of the natural abundance of Li (Meija et al., 2016). Stable isotope values are reported in per mille (‰) notation of the deviation from an accepted standard reference material, which for Li isotopes is NIST SRM 8545 (LSVEC, Li-carbonate) with an accepted $^7\text{Li}/^6\text{Li}$ value of 12.0192 \pm 0.0002 (Flesch et al., 1973).

$$\delta^{7} \text{Li \%}_{o} = \left(\frac{R_{Sample} - R_{Standard}}{R_{Standard}}\right) \times 1000 \tag{1}$$

where $R = {}^{7}\text{Li}/{}^{6}\text{Li}$.

Table 2Lithium isotope results for U.S source rocks of different organic Types.

Sample	State	Age	VRo %	δ7Li ‰ ± S.E.	n	Organic Type
Hydrocarbon source rocks						
¹ Wilcox Fm. Lignite	TX	Lower Eocene	0.45	-19.8 ± 2.4	4	III
² Bakken Fm. Lower Bakken Mbr	ND	Mississippian	0.50	-8.8 ± 1.9	8	I/II
³ Green River Fm.	WY	Eocene	0.65	-15.0 ± 3.6	4	I
⁴ New Albany Fm. Blocher Mbr.	IL	Mississippian	0.95	-0.9 ± 2.2	8	II

Lithium isotope compositions determined by IMS-6f, where n = number of analyses on each sample; S.E. – 1 σ standard error; nr – not reported; VRo - vitrinite reflectance values %; VRo values for Wilcox, Green River and New Albany shales are estimated from: ¹Mukhopadhyay, 1994; ²Canter et al., 2016; ³Pawlewicz and Finn, 2002; ⁴East et al., 2012; ⁴Lewan et al., 1995; ⁴Nuccio and Hatch, 1996.

^{*} Indicates VM dry basis; Vit- Vitrinite % (Matthews and Pisupati, 2018; Palmer, 1997; Vorres, 1990).

2.4. Secondary ion mass spectrometry

Two different SIMS instruments, the Cameca Ametek Ion Mass Spectrometer (IMS-6f) and NanoSIMS 50 L (NanoSIMS) were used to obtain in situ Li isotopic ratios of samples. Both instruments have duoplasmatron sources which generate a plasma beam of O⁻ ions. The primary beam is focused to a spot on the sample surface. This high energy ion bombardment sputters the sample surface ejecting ions, atoms, and electrons (Hervig, 1996). Positive secondary ions, such as ⁷Li⁺ and ⁶Li⁺, are transmitted through a series of lenses and apertures in the secondary column and separated by energy in an electrostatic analyzer. Ions are differentiated by their mass (m) to charge (z) ratio in the mass spectrometer and are detected using either an electron multiplier or faraday cup. For our analyses, all ions were detected using electron multipliers, calibrated using internal reference standards. Mass interferences must be eliminated by using energy filtering (for molecular interferences) or by adjusting the entrance and exit slits (or apertures) to the mass spectrometer to increase the mass resolving power (MRP = mass/ Δ mass). Primary interferences were ²⁴Mg²⁺ and ¹¹BH⁺ interfering with ¹²C⁺. The ¹⁴N²⁺ signal was easily resolved from ⁷Li, and sufficient MRP was used on both instruments to resolve m/z interferences.

To determine the instrumental mass fractionation (IMF) we used several standard reference materials (NIST SRM 610, NIST SRM 612), and illite from the Clay Minerals Society Source Clay Repository (IMt-1; www.clays.org). Each of these standards verified consistent values of IMF (mean daily S.E. \pm 1.0%, 1 σ) and standard bracketing of unknowns, with one or more of these internal reference materials, was used to monitor instrumental drift during each analytical session (See Supplement material (SM) Fig. S1).

SIMS measurements are subject to matrix effects, where ions sputter at different rates (cps) from different matrices (Burnett et al., 2015; Hauri et al., 2006; Seah and Shard, 2018). We acknowledge that compositional differences between standards and unknowns (e.g., silicates vs. organics) may lead to matrix effects on the ionization process, which could shift the isotopic ratios measured (Hauri et al., 2006). For example, Bell et al. (2009) found that changes in Mg-content of olivine affected the $\delta^7 \text{Li}$ values by 1.3% per mole Mg substituted. There is not yet a kerogen standard with known Li isotopic composition verified by alternative analytical techniques. However, we suggest that δ^7 Li values within a kerogen Type class (I, II or III) will be comparable as their major element compositions are similar (e.g., Ishida et al., 2018). Furthermore, we found no correlation between $\delta^7 Li$ and the C-H-O contents of measured Type III kerogen in coals (SM; Figs. S6-S8). There is also no standard for calibration of Li contents in kerogen matrices but the $^7\text{Li}/^{12}\text{C}$ intensity ratio can be used to compare relative abundances among similar phases (e.g., Type III kerogen).

2.4.1. IMS-6f analytical protocol

The primary beam current and ion optics determine the beam diameter and therefore the analysis spot size. For the IMS-6f, the duoplasmatron source generates a primary beam of O $^-$ ions at $-12.5~\rm kV$ and the sample is held at $+9.0~\rm kV$ for a total impact energy of 21.5 kV. The spot size can be as small as a few microns ($\sim 5~\rm \mu m)$ in diameter, but in samples with low Li content, higher currents were necessary to provide enough Li $^+$ secondary ions counts for statistical significance. Generally, a 5–20 nA primary current yielding a beam diameter of $<50~\rm \mu m$ was used for spot analyses on all samples measured by IMS-6 f. Ions with an energy range $\pm~20~\rm eV$ were allowed into the secondary magnet where the magnetic field can be adjusted to select the m/z of interest. For the IMS-6f analyses, each sample was analyzed on multiple spots as indicated in Tables 1 and 2 ($n=2~\rm to$ 33). The IMF measured before and after analysis of unknowns was used to correct the raw isotope ratios.

2.4.2. NanoSIMS analytical protocol

A duoplasmatron source was also used for NanoSIMS measurements, generating a plasma beam of O $^-$ ions at -8 kV. The sample is held at +8 kV for a total impact energy of 16 kV. The NanoSIMS design uses a smaller primary beam of tens to hundreds pA of O $^-$, to achieve greater spatial resolution than the IMS-6 f. The advantage of NanoSIMS is the ability to make ion images of the distribution of isotopes over a small area (typically 5–25 μm^2) and at a greater spatial resolution. This allows spatial separation of measurements in the kerogen matrix avoiding silicate minerals (e.g., clays) in the kerogen matrix.

For the NanoSIMS analyses, ion maps were made in the imaging mode by rastering the beam over $25\mu m^2$ areas to measure the distribution of ⁷Li⁺, ¹²C⁺ and ³⁰Si⁺ (cps). Images were taken at two different pixel resolutions (256 \times 256 and 512 \times 512) and varying spatial resolutions with beam diameter ranging from ~ 300 nm to 2 μm (3 pA – 500 pA primary current). All images were taken with a counting time of 1000 µs/pixel. NanoSIMS real time imaging was used in conjunction with the ion maps to pinpoint regions of interest (ROI) within the rastered area where the ¹²C⁺ or ³⁰Si⁺ signals were high. Maps of ¹⁴N⁺, ²⁴Mg⁺, ³⁹K⁺, and ⁴⁰Ca⁺ ions were also made to help identify the matrix being measured, e.g., determining if a spot with relatively high ¹²C⁺ counts was kerogen or a carbonate mineral, differentiating Kbearing clays vs. quartz, and to confirm that the $^{24}{\rm Mg}^{2+}$ m/z was not interfering with the 12C+ m/z measurements. Using a primary beam current of 100–500 pA with a beam diameter of 1–3 μm we measured Li isotopic ratios in areas of high- $^{12}C^+$ versus high- $^{30}Si^+$ (cps). Using this protocol, we were able to separate analyses of kerogen and silicate phases and acquire their Li isotopic compositions at high spatial resolution.

3. Results

A histogram of all measurements of $\delta^7 \text{Li}$ by IMS-6f and NanoSIMS instruments for coals and source rocks is shown in Fig. 3. Multiple SIMS measurements on each sample were averaged and are summarized in Tables 1 and 2. The individual analyses and statistical evaluation can be found in Table S1. The $\delta^7 \text{Li}$ values measured are mostly < 0‰, except where analyses possibly overlapped silicates. We also characterized spot measurements according to their $^{12}\text{C}/^{30}\text{Si}$ ratios and defined Sirich areas where $^{12}\text{C}/^{30}\text{Si}$ < 1.0, while C-rich areas ranged from $^{12}\text{C}/^{30}\text{Si}$ = 1 to 12,000. For Si-rich areas (n = 28) the average $\delta^7 \text{Li}$ is

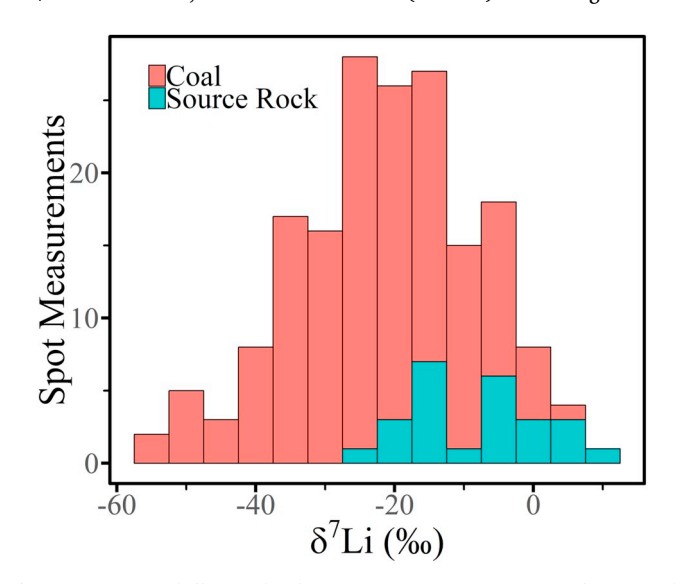


Fig. 3. Histogram of all IMS-6f and NanoSIMS spot measurements taken on coal and source rock samples. Coal samples generally had lower $\delta^7 \text{Li}$ than source rocks which may be because of beam overlap of kerogen and silicates during source rock measurements.

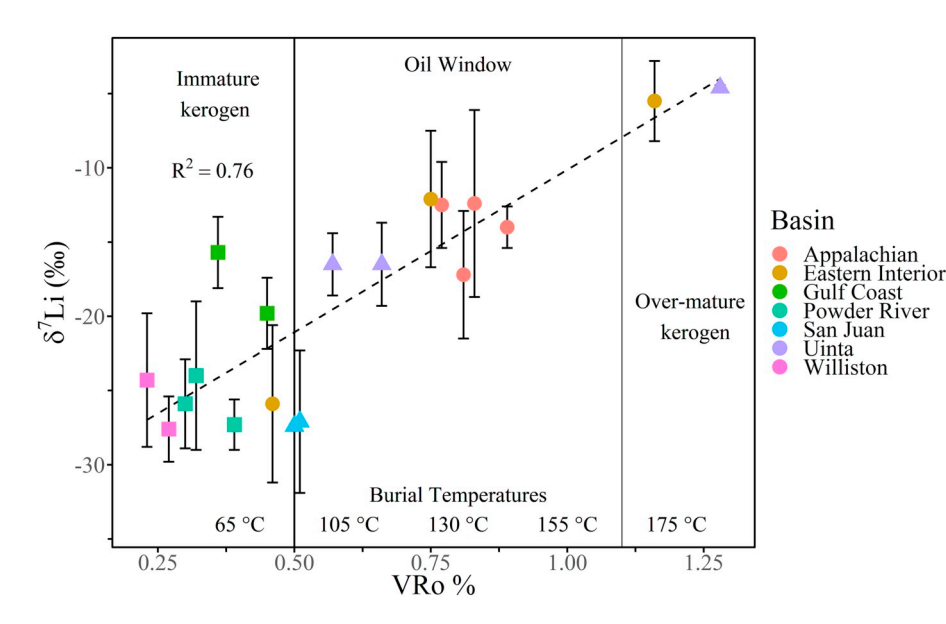


Fig. 4. Vitrinite reflectance in oil (VRo %) is plotted against the Li isotope ratios of coal samples. Each point represents the mean value for multiple (n) measurements of a single sample. Error bars indicate 1σ standard error of n analyses (see Table 1; all data shown in Table S1). Two samples have error bars smaller than the point. Burial temperatures were estimated based on VRo % (Barker and Goldstein, 1990; Bostick, 1979; Burnham and Sweeney, 1989). Symbols indicate age; Tertiary (squares), Cretaceous (triangles) and Carboniferous (circles). There is a positive correlation between $\delta^7 \text{Li}$ and VRo % of measured coals.

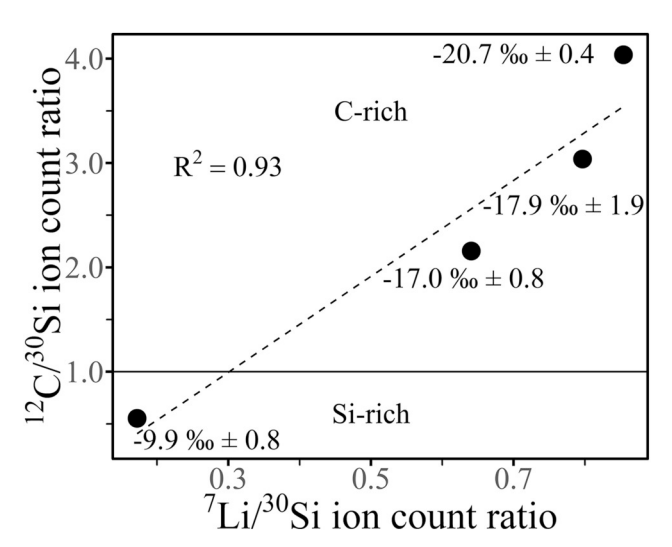


Fig. 5. Measurements on Green River Shale sample using IMS-6 f. The $\delta^7 \text{Li}$ values are indicated beside each analysis. C-rich spots are isotopically lighter than Si-rich spots. Standard errors are smaller than the symbols.

 $-7.3\pm1.7\%$, and for C-rich areas (n=130) the average $\delta^7 {\rm Li}$ is $-23.6\pm1.1\%$ (Fig. S9). Each coal sample (Table 1) was measured in multiple spots (n=2-33) and the mean and standard error of the mean for all analyses on each sample is plotted in Fig. 4. The variability in measurements from spot to spot within a single sample may be due to heterogeneity of the various organic macerals, beam overlapping multiple phases (kerogen and silicates), sample charging, or surface roughness of pressed powders. Nonetheless, the average analytical error on each spot analysis was 1.1% (1σ) which is far less than the observed range of values (SM; Table S1).

The source rock samples from the Green River Fm., New Albany Fm. and Wilcox Fm were measured by IMS-6f and the Lower Bakken shale sample was measured by both IMS-6f and NanoSIMS. Given the range of VRo values reported for these source rocks (Table 2), the more thermally mature New Albany shale has the highest $\delta^7 Li$ values, while the less mature source rocks have lower $\delta^7 Li$ values on average. Spot analyses in the Green River Fm. (Type I) showed a correlation (R² = 0.93) between $^7 Li/^{30} Si$ ratios and $^{12} C/^{30} Si$ ratios (Fig. 5) with isotopically lighter values observed in C-rich spots.

3.1. NanoSIMS imaging of Bakken Shale

NanoSIMS ion maps and nanometric spot measurements of $^6\text{Li}^+$, $^7\text{Li}^+$, $^{12}\text{C}^+$, $^{30}\text{Si}^+$, were made on immature (VRo 0.5%) samples of the Mississippian Lower Bakken Shale to discriminate isotopic differences between kerogen and mineral matrices (Fig. 6). Regions of interest (ROI) circled in white had high C counts and ROI circled in red had high Si counts, relative to other regions in that image, and were selected for precise spot analyses of Li isotopes. The 8^7Li values are labeled next to each ROI on the $^7\text{Li}^+$ ion maps. Regions dominated by ^{12}C , generally showed lower 8^7Li values than regions with higher $^{30}\text{Si}^+$ counts. One isotopic measurement (Fig. 6D; spot 2) had a positive value (+11.2%) and notably the $^7\text{Li}^+$ in this region was spatially correlated with $^{39}\text{K}^+$ ions. This suggests that the isotopically heavy Li was from a K-bearing mineral (e.g., feldspar or clay).

4. Discussion

4.1. Coal survey of δ^7 Li

Few studies have examined the organic vs. mineral hosts of Li in coal, although some bulk measurements of Li in coals have reported that Li is hosted by the silicates or "ash" portion (Finkelman, 1980; Dai et al., 2012). Our in situ study of Li in coals shows no correlation between δ^7 Li and the contents of elements commonly associated with ash (Si, Al, K) for measured APCS and DECS coals (SM; Figs. S3-S5). Swaine (1990) stated that Li is partly associated with organic matter, and Finkelman et al. (2018) later reported up to ~50% of Li in immature coals may be associated with organic material. Terrestrial plant matter that is the primary component of coals is one possible source of organolithium compounds. Gough et al. (1977) found the Li content of plants to be positively correlated with the Li content of the soils in which they grew. Li has a varying toxicity threshold among plants depending on the species, yet plants contain trace amounts of Li (0.01-31 ppm) on average (Pendias and Kabata-Pendias, 2000). Leguminous plants grown in Li rich soils (9-175 ppm) in New Zealand are reported to contain up to 143 ppm Li (Pendias and Kabata-Pendias, 2000). Beets can take up even higher amounts of Li (up to 5500 ppm) from Li-rich soils and have been proposed for agro-mining (Kavanagh et al., 2018). Even though Li is present in small concentrations in most plants, it can become concentrated during the formation of kerogen due to the breakdown of biomolecules and consolidation of plant material during burial and lithification. Littke and Leythaeuser (1993) found that a 1-m thick layer of peat generates ~20 cm of bituminous coal,

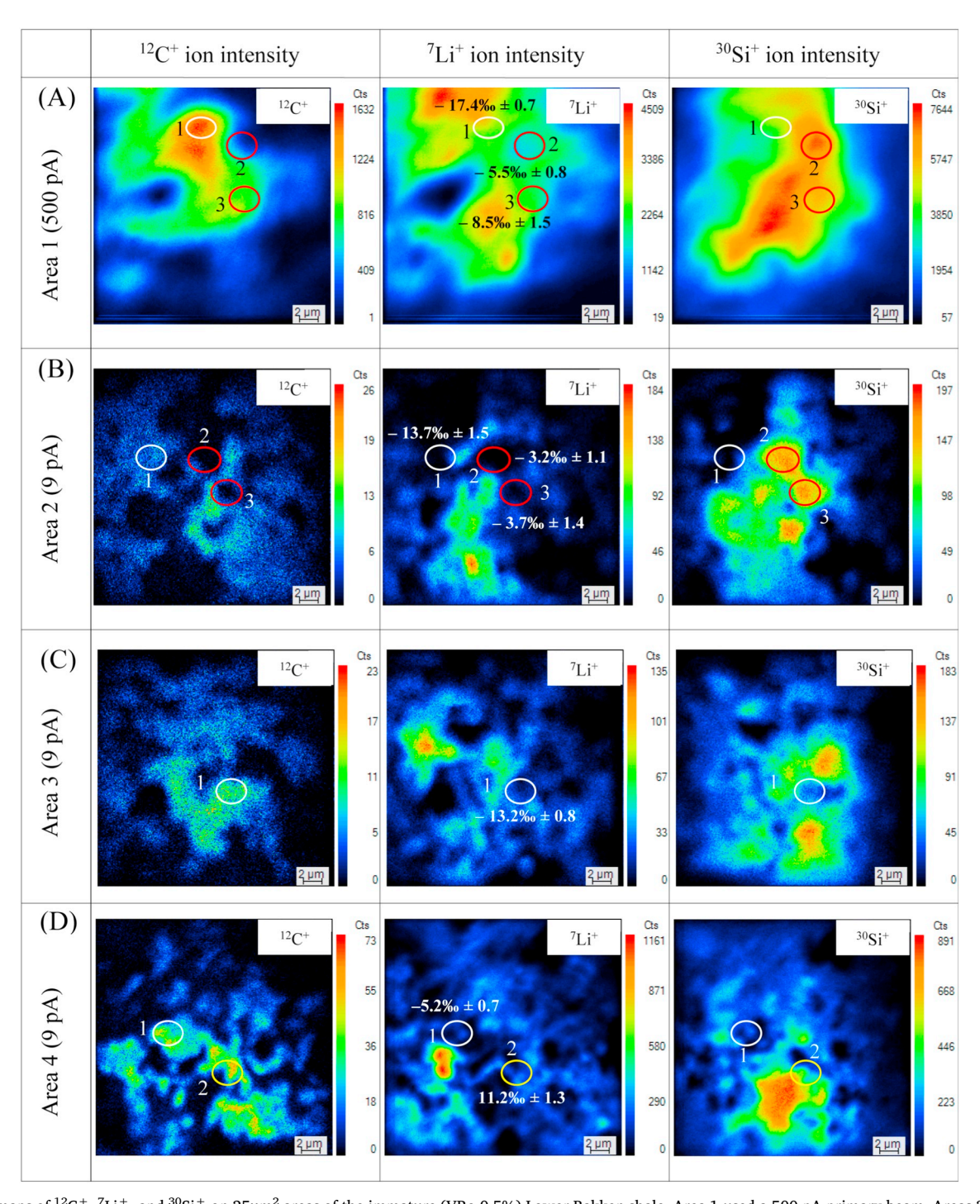


Fig. 6. Ion maps of $^{12}C^+$, $^7Li^+$, and $^{30}Si^+$ on $25\mu m^2$ areas of the immature (VRo 0.5%) Lower Bakken shale. Area 1 used a 500 pA primary beam, Areas 2–4 used a 9 pA beam to increase spatial resolution, at the expense of secondary ion counts. One scan was taken for all images apart from Area 4 (Fig. 6D) which is an accumulation of 20 scans which were corrected for drift and summed. Circled areas show high ^{12}C (white), high ^{30}Si (red) or mixed ^{12}C and 30Si (yellow) spots where δ^7Li measurements were made; values shown on the 7Li -map. ROI with high ^{12}C have lower δ^7Li values than high ^{30}Si ROI. (For interpretation of the references to colour in this figure legend, the reader is referred to the web version of this article.)

therefore 3 ppm Li in peat can produce a coal with 15 ppm Li.

The range of Li isotopes published for various terrestrial and extraterrestrial samples is summarized in Fig. 2 (Clergue et al., 2015; Lemarchand et al., 2010; Négrel et al., 2010; Penniston-Dorland et al., 2017; Tomascak et al., 2016). The coals measured in this study represent the lowest $\delta^7 \text{Li}$ values measured, typically < 0% for the most organic-rich samples. This range of $\delta^7 \text{Li}$ values is similar to the range of $\delta^{11} \text{B}$ values measured on these same coal samples (Williams and Hervig, 2004). The low $\delta^7 \text{Li}$ values in low rank coals suggest that immature

organic macerals in the coal are enriched in ⁶Li compared to most rocks, minerals and waters evaluated in the global geochemical cycle (Fig. 2).

Consistent with our Li isotope results for kerogens, other studies of Li isotopes in organic materials have reported isotopically light $\delta^7 \text{Li}$ values. Lemarchand et al. (2010) found forest soil solutions as well as fir tree needles, branches and roots to $\delta^7 \text{Li}$ values lower (-5 to -17%) than the parent granite (+0.3%), soil (+0.7 to +3.3%) and stream waters (+5 to +20%) in a forested granitic catchment in France. Another study on peat from the Massif Central in France (Négrel et al.,

2010) reported δ^7 Li values of -11 to 0‰.

Only two studies have reported $\delta^7 \text{Li}$ of coal constituents. Harkness et al. (2015) measured $\delta^7 \text{Li}$ values from -7 to +12.8% for aqueous leachates of the inorganic constituents of coals from the Powder River, Appalachian and Eastern Interior basins. He et al. (2019) used microwave digested coal samples from the high Li, (> 500 ppm) Guanbanwusu mine (China) and reported $\delta^7 \text{Li}$ values from +6 to +8% on residues measured by ICP-MS. The anomalously high Li contents of this coal have been shown to be positively correlated with the ash content suggesting secondary Li enrichment from a hydrothermal source (Sun et al., 2012). Therefore, the somewhat heavier lithium isotope compositions reported for this Guanbanwusu coal are likely controlled by the silicate hosted minerals.

Our results show a clear positive correlation ($R^2 = 0.76$) between δ⁷Li of coals and thermal maturity as indicated by VRo (Fig. 4). Low rank coals (VRo < 0.5%) have the lowest $\delta^7 \text{Li}$ values (average $-23.4 \pm 1.1\%$) and the Li isotope composition becomes heavier (up to -5%) with increasing rank up to VRo $\sim 1.3\%$ (bituminous), irrespective of age and depositional environment (Table 1). The observation that δ^7 Li values of kerogen in coals become higher as thermal maturity increases may be interpreted as either a preferential release of ⁶Li to pore fluids as temperature increases, or an uptake of ⁷Li from hydrothermal fluid during thermal maturation. However, no clear correlation was observed between Li/C and either VRo or δ^7 Li (SM; Fig. S2). Given that these samples each come from many different sedimentary basins of varying geological ages, they each have their own initial Li contents and diagenetic histories that would affect the Li/C ratios. Kerogen from different ages spanning 300 Myr may come from plants with varying Li contents. Considering that a positive trend is shown among all coals studied, it is most likely that the trend reflects a preferential loss of ⁶Li rather than incorporation of exogenous ⁷Li. While hydrothermal Li certainly influences some basins (e.g., Dai et al., 2012), if this were the case ubiquitously, we would expect higher Li/C ratios in hydrothermally influenced (more mature) samples, which is

The trend of increasing 8^7Li with thermal maturity is consistent with a previous study showing $^6 \text{Li}$ enrichment in authigenic clays associated with the migration of gas into the Wattenberg gas field, Denver Basin (Williams et al., 2015). That study proposed that $^6 \text{Li}$ preferentially leaves organolithium compounds during gas generation from kerogen (VRo > 1.5%). Different kerogen Types generate hydrocarbons (oil and gas) over a range of burial temperatures. The 'oil window' spans a VRo range from 0.50 to 1.35% (Hunt, 1996; Mukhopadhyay, 1994; Peters and Cassa, 2007; Pittion and Gouadain, 1985; Taylor et al., 1998; Tissot et al., 1987; Tissot and Welte, 1984). On the other hand, Type III kerogen (coals) have an effective 'oil window' at VRo values of 0.65–2.0% with gas generation dominant above VRo 1.5% (Petersen, 2006). The trend in 8^7Li values of coals (Fig. 4) clearly coincides with the temperatures of hydrocarbon generation from kerogen, supporting a preferential release of $^6 \text{Li}$ to hydrocarbon-related fluids.

Interestingly, we measured two over mature samples APCS-6 from UT (VRo 1.68%) and DECS-21 from PA (VRo 5.19%) that fell off the trendline demonstrated by other coals. These samples show very low $\delta^7 {\rm Li}$ values ($-22~\pm~0.8$ and $-~39~\pm~4.0\%$, respectively; Table 1). Clearly at very high temperatures, the coal remaining is largely residual C and ash. It is possible that at very high thermal maturity, most of the organolithium compounds have been degraded (released) during hydrocarbon generation, and that any remaining Li is hosted by silicates, or residual C.

4.2. Hydrocarbon source rocks

Oil and gas are generated from source rocks at temperatures between $\sim\!60\text{--}150~^\circ\text{C}$, generally at burial depths from 1 to > 4 km. The hydrocarbons can be expelled from source rocks and migrate along pathways through permeable rock into structural and stratigraphic

traps, forming conventional hydrocarbon reservoirs. Black shale source rocks can also host oil and gas forming unconventional reservoirs. Therefore, a distinctly light Li isotopic composition of pore fluids, suggesting influx of hydrocarbon-sourced Li, may be useful in identifying productive intervals of a shale. We studied several well-known hydrocarbon source rocks to compare the Li isotopic compositions of their different kerogen Types.

It was recognized while measuring source rocks with the IMS-6f instrument, that the large (up to $50 \mu m$) primary ion beam diameter on the IMS-6f and the predominance of silicates over kerogen in source rocks influenced analyses where kerogen and silicate analyses overlapped. This resulted in slightly more positive δ^7 Li values in the shale source rocks than coals (Fig. 3), which are dominated by carbonaceous material (ASTM Committee, 2019), thus decreasing overlap on minerals. Primary beam overlap on silicates was avoided using the NanoSIMS on the Bakken shale sample, so that Li isotope measurements could be compared between kerogen and mineral phases (Section 3.1). The Mississippian Lower Bakken shale was studied in detail because it is a Type I/II source rock with high total organic carbon (up to 35 wt%; Jin and Sonnenberg, 2012). NanoSIMS maps of the Bakken shale (Fig. 6) and IMS-6f measurements of Green River Fm. (Fig. 5) showed that the C-rich areas have isotopically lower δ^7 Li values than Si-rich areas of the source rocks. Like the coal measurements, immature kerogen in source rocks contains isotopically light Li (Table 2). The general trend for source rock kerogen similarly shows δ^7 Li values increasing with thermal maturity over the temperature range of oil and gas generation.

4.3. Implications for Li geochemical cycles

The results presented here support the idea that Li derived from kerogen can be used to trace organic-related fluids because the Li isotopic composition of pore waters from kerogen should be lighter than most other natural waters (Fig. 2). Oilfield brines generally range from δ^7 Li + 4 to + 16‰ (Eccles and Berhane, 2011; Macpherson et al., 2014; Millot et al., 2011; Phan et al., 2016), except where evaporative processes enrich the brines in ⁷Li (Chan et al., 2002) (SM Table S2). These brines are lighter than seawater ($\delta^7 \text{Li} \sim 31\%$) (Chan and Edmond, 1988; Misra and Froelich, 2012), rivers (mean = +23%), and lakes (+17 to +36). Hydrocarbon-related fluids contain elevated contents of many organically derived trace elements (e.g., Li, B, N) and many of these elements are substituted into authigenic clays that form under diagenetic conditions affecting coals and hydrocarbon sources (Williams et al., 2012, 2013, 2015). Given that up to 50% of Li in immature coals may be associated with kerogen (Finkelman et al., 2018) and the observation that more mature bituminous coal contains Li associated with the silicates (ash) (Finkelman et al., 2018), we hypothesize that the Li is released from dispersed organic matter and becomes concentrated in authigenic clays. Among coals surveyed by Finkelman et al. (2018), 6 immature coals contained on average only ~6 ppm Li while 14 bituminous (mature) coals contain on average 44 ppm Li. If Li accumulates in pore fluids during burial, then the pore fluids become enriched in the Li released from organolithium complexes in the source

The isotopic fractionation as Li is released from organic compounds in kerogen to pore fluid is unknown, but the isotopic fractionation of Li between water and authigenic clays (smectite-illite) is well-known (Wunder et al., 2007; Vigier et al., 2008; Williams et al., 2012). Therefore, where temperatures can be constrained, assuming equilibrium conditions, the Li isotopic composition of the fluid can be calculated. For example, the $\delta^7 {\rm Li}$ of the high Si area in the Bakken shale (Fig. 6; Area 1; ROI-2) gave a value of -5.5%. High $^{39}{\rm K}$ in this area suggests that this may be illite (or possibly a detrital feldspar). Using the isotopic fractionation equation determined for illite-water fractionation:

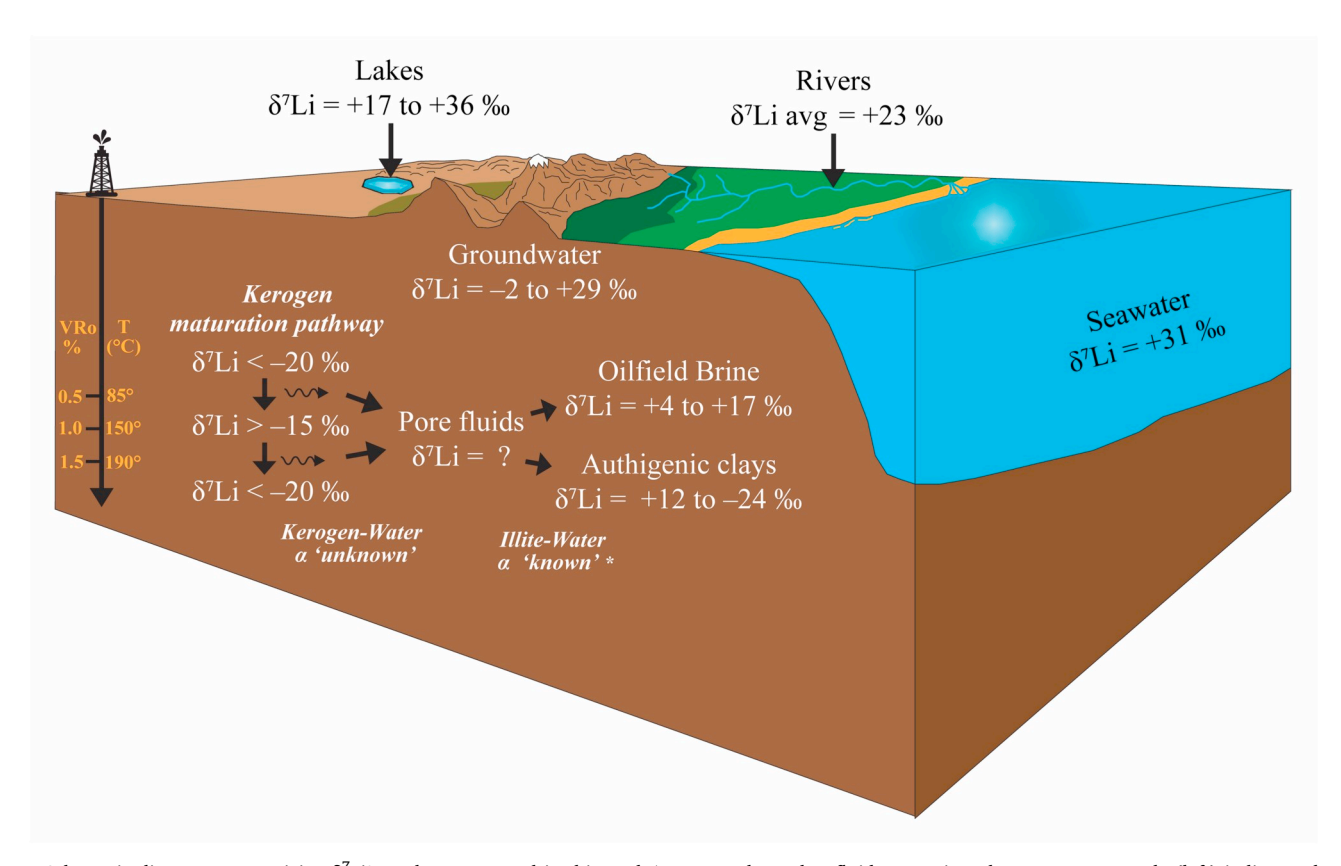


Fig. 7. Schematic diagram summarizing $\delta^7 \text{Li}\%$ values measured in this study* compared to other fluid reservoirs. The temperature scale (left) indicates the 'oil window' (VRo from 0.5 to 1.5%) where heavier $\delta^7 \text{Li}\%$ values may include exogenous Li in nanopores. In general, Li released from kerogen is enriched in ⁶Li, as reflected by isotopically light oilfield brines. The distinctly light isotopic compositions derived from kerogen can be incorporated into authigenic clays to trace organic inputs to fluids. (Sources: this study; Macpherson et al., 2014; Penniston-Dorland et al., 2017; Tomascak et al., 2016; Williams and Hervig, 2005*).

1000 ln
$$\alpha = 6.15 - 0.07(1000/T (K))$$
 (2)

(Williams et al., 2012) and estimating a temperature $\sim 80\,^{\circ}\text{C}$ based on the vitrinite reflectance of the Bakken immature kerogen, one can calculate a pore fluid $\delta^{7}\text{Li}$ value of +14.5%, which is in the range of other natural ground waters (Fig. 2). Realistically, the measured $\delta^{7}\text{Li}$ measured (Fig. 6; Area 1; ROI-2) includes interlayer Li in addition to structurally bound Li in the clay, so this value may be slightly heavier than the water that equilibrated with the authigenic clay (Williams et al., 2015). Evaluating the isotopic fractionation of Li between kerogen and water will be useful in refining the potential use of Li isotopes for tracing hydrocarbon migration paths through organic-rich shales.

Another important implication for this work is its impact on interpretations of continental weathering based on δ^7 Li values. For example, the Li isotopic composition of seawater over the Cenozoic era has been interpreted to have been lighter in the past due to high rates of continental weathering based on the δ^7 Li of foraminifera (Misra and Froelich, 2012) and other biogenic carbonate (Sun et al., 2018). While the trend of decreasing δ^7 Li in foraminifera over the Cenozoic era is robust, the effects of diagenesis on the re-equilibration of carbonate δ^7 Li with diagenetically altered fluids, might warrant reconsideration in light of our data showing distinctly light Li isotopic compositions of kerogen. It is possible that increased nutrient supplies to the ocean, associated with high erosion rates, caused eutrophication and hypoxia, and these conditions led to preservation of sedimentary organic matter (Gallois, 1976; Liu and Wang, 2013; Loftus and Greensmith, 1988). Therefore, the low δ^7 Li values recorded by deeply buried forams, where diagenesis is likely, may be reflecting the isotopic composition of organic-derived Li on paleofluid compositions. Understanding the exchange of Li between organic matter, fluids and minerals in sedimentary basins contributes not only to our understanding of hydrocarbon generation and migration, but also to the evaluation of Li sources important to the global Li geochemical cycle.

5. Conclusions

Our survey of Li isotopic compositions in organic rich rocks of varying depositional environment, age, and thermal maturity leads to the following insights:

- Immature kerogen measured in this study has a lighter Li isotopic composition than any other crustal material (mineral or fluid) yet reported.
- 2. With increasing thermal maturity, from immature to mature (up to VRo 1.3%), the δ^7 Li values of kerogen increase. We conclude that 6 Li is preferentially released from the organic matrix to pore fluids during thermal maturation.
- 3. The organic matrix in hydrocarbon source rocks has a lighter Li isotopic composition than the silicate matrix.
- 4. If Li released from kerogen is isotopically light relative to most pore fluids, then the uptake of Li from these fluids by authigenic clays will record the isotopically light Li related to hydrocarbon generation.
- The recognition of isotopically light Li derived from organic sources could impact interpretations of continental weathering and should be further investigated for its significance in the global geochemical cycle.

Supplementary data to this article can be found online at https://doi.org/10.1016/j.chemgeo.2020.119694.

Declaration of competing interest

The authors declare that they have no known competing financial interests or personal relationships that could have appeared to influence the work reported in this paper.

Acknowledgements

We thank Cortland Eble (Kentucky Geological Survey) for petrographic and proximate analysis of coal samples, the Salt River Materials Group and Westmoreland Savage mine for coal samples, Michael Lewan of the US Geological Survey and Lyn Canter of Whiting Petroleum Corporation for source rock samples, Ziliang Jin for NanoSIMS assistance and Rick Hervig for valuable advice on the analytical protocol.

Funding

This work was funded by the National Science Foundation (EAR-1811613) and analytical work was supported by the ASU SIMS Facility funded by (EAR-1352996).

References

- Akar, C., 2014. Maturity and Hydrocarbon Potential of the New Albany Shale and Maquoketa Shale in the Illinois Basin, USA (M.S.). Indiana University, United States – Indiana.
- Albert, S., 2014. Sedimentology, Facies Architecture and Sequence Stratigraphy of the Lower Bakken Shale Member in the Williston Basin, North Dakota, United States of America. Colorado State University, Fort Collins, CO, pp. 47 Unpublished M.S. thesis.
- ASTM Committee, 2019. Classification of Coals by Rank (No. ASTM D388–19). ASTM International, 100 Barr Harbor Drive, PO Box C700, West Conshohocken, PA 19428–2959, United States. https://doi.org/10.1520/D0388-19.
- Barker, C.E., Goldstein, R.H., 1990. Fluid-inclusion technique for determining maximum temperature in calcite and its comparison to the vitrinite reflectance geothermometer. Geology 18, 1003–1006. https://doi.org/10.1130/00917613(1990) 018 < 1003:FITFDM > 2.3.CO; 2.
- Bell, D.R., Hervig, R.L., Buseck, P.R., Aulbach, S., 2009. Lithium isotope analysis of olivine by SIMS: Calibration of a matrix effect and application to magmatic phenocrysts. Chem. Geol. 258, 5–16. https://doi.org/10.1016/j.chemgeo.2008.10.008.
- Bostick, N.H., 1979. Microscopic measurement of the level of catagenesis of solid organic matter in sedimentary rocks to aid exploration for petroleum and to determine former burial temperatures—a review, in: Scholle, P.A., Schluger, P.R. (Eds.), Aspects of Diagenesis, SEPM Special Publication. Society for Sedimentary Geology. vol. 26. doi:https://doi.org/10.2110/pec.79.26.0017.
- Bottomley, D.J., Katz, A., Chan, L.H., Starinsky, A., Douglas, M., Clark, I.D., Raven, K.G., 1999. The origin and evolution of Canadian Shield brines: evaporation or freezing of seawater? New lithium isotope and geochemical evidence from the Slave craton. Chem. Geol. 155, 295–320. https://doi.org/10.1016/S0009-2541(98)00166-1.
- Bottomley, D.J., Chan, L.H., Katz, A., Starinsky, A., Clark, I.D., 2003. Lithium Isotope Geochemistry and Origin of Canadian Shield Brines. Groundwater 41, 847–856. https://doi.org/10.1111/j.1745-6584.2003.tb02426.x.
- Bradley, W.H., 1931. Origin and microfossils of the oil shale of the Green River formation of Colorado and Utah. US Geol. Surv. Prof. Pap. 168, 57.
- Bregg, L.J., Oman, J.K., Tewalt, S.J., Oman, C.L., Rega, N.H., Washington, P.M., Finkelman, R.B., 1998. U.S. Geological Survey Coal Quality (COALQUAL) Database: Version 2.0 (Open-File Report No. OF-97-134). U.S. Geological Survey, Denver, CO. https://ncrdspublic.er.usgs.gov/coalqual/.
- Burnett, D.S., Jurewicz, A.J.G., Woolum, D.S., Wang, J., Paque, J.M., Nittler, L.R., McKeegan, K.D., Humayun, M., Hervig, R., Heber, V.S., Guan, Y., 2015. Ion implants as matrix-appropriate calibrators for geochemical ion probe analyses. Geostand. Geoanal. Res. 39, 265–276. https://doi.org/10.1111/j.1751-908X.2014.00318.x.
- Burnham, A.K., Sweeney, J.J., 1989. A chemical kinetic model of vitrinite maturation and reflectance. Geochim. Cosmochim. Acta 53, 2649–2657. https://doi.org/10.1016/ 0016-7037(89)90136-1.
- Canter, L., Zhang, S., Sonnenfeld, M., Bugge, C., Guisinger, M., Jones, K., 2016. Chapter 2: Primary and secondary organic matter habit in unconventional reservoirs. In: Imaging Unconventional Reservoir Pore Systems. AAPG Memoir 112pp. 9–23. https://doi.org/10.1306/M1121309.
- Chan, L.H., Edmond, J.M., 1988. Variation of lithium isotope composition in the marine environment: a preliminary report. Geochim. Cosmochim. Acta 52, 1711–1717. https://doi.org/10.1016/0016-7037(88)90239-6.
- Chan, L.-H., Starinsky, A., Katz, A., 2002. The behavior of lithium and its isotopes in oilfield brines: evidence from the Heletz-Kokhav field, Israel. Geochim. Cosmochim. Acta 66, 615–623. https://doi.org/10.1016/S0016-7037(01)00800-6.
- Clergue, C., Dellinger, M., Buss, H.L., Gaillardet, J., Benedetti, M.F., Dessert, C., 2015. Influence of atmospheric deposits and secondary minerals on Li isotopes budget in a highly weathered catchment, Guadeloupe (Lesser Antilles). Chem. Geol. 414, 28–41. https://doi.org/10.1016/j.chemgeo.2015.08.015.

Collins, A.G., 1975. Chapter 5. Significance of some inorganic constituents and physical properties of oilfield waters. In: Developments in Petroleum Science. Elsevier, pp. 133–176. https://doi.org/10.1016/S0376-7361(08)70198-5.

- Cronin, J.R., Pizzarello, S., Frye, J.S., 1987. 13C NMR spectroscopy of the insoluble carbon of carbonaceous chondrites. Geochim. Cosmochim. Acta 51, 299–303. https://doi.org/10.1016/0016-7037(87)90242-0.
- Dai, S., Jiang, Y., Ward, C.R., Gu, L., Seredin, V.V., Liu, H., Zhou, D., Wang, X., Sun, Y., Zou, J., Ren, D., 2012. Mineralogical and geochemical compositions of the coal in the Guanbanwusu Mine, Inner Mongolia, China: further evidence for the existence of an Al (Ga and REE) ore deposit in the Jungar Coalfield. Int. J. Coal Geol. 98, 10–40. https://doi.org/10.1016/j.coal.2012.03.003.
- Durand, B., 1980. Kerogen, Insoluble Organic Matter from Sedimentary Rocks. Graham and Troman, Paris (519p).
- East, J., Swezey, C., Repetski, J., Hayba, D., 2012. Thermal Maturity Map of Devonian Shale in the Illinois, Michigan, and Appalachian Basins of North America. In: Scientific Investigations Map, https://pubs.usgs.gov/sim/3214/pdf/sim3214.pdf.
- Eccles, D.R., Berhane, H., 2011. Geological Introduction to Lithium-Rich Formation Water with Emphasis on the Fox Creek Area of West-Central Alberta (NTS 83F and 83K) (Open File Report). Energy resources Conservation Board, Alberta, Canada. https://ags.aer.ca/document/OFR/OFR_2011_10.pdf.
- Finkelman, R.B., 1980. Modes of Occurrence of Trace Elements in Coal. University of Maryland, College Park, Maryland, pp. 172 Unpublished Ph.D. Dissertation.
- Finkelman, R.B., Palmer, C.A., Wang, P., 2018. Quantification of the modes of occurrence of 42 elements in coal. Int. J. Coal Geol. 185, 138–160. https://doi.org/10.1016/j.
- Flesch, G.D., Anderson, A.R., Svec, H.J., 1973. A secondary isotopic standard for ⁶Li/⁷Li determinations. Int. J. Mass Spectrom. 12, 265–272. https://doi.org/10.1016/0020-7381(73)80043-9.
- Gallois, R.W., 1976. Coccolith blooms in the Kimmeridge Clay and origin of North Sea Oil. Nature 259, 473–475. https://doi.org/10.1038/259473b0 doi:10.1016/j.chemgeo. 2019.119340.
- Gough, L., Shacklette, H., Case, A., 1977. Element Concentrations Toxic to Plants, Animals, and Man. U.S., Geol Surv Bull 1466. pp. 78. https://pubs.usgs.gov/bul/ 1466/report.pdf.
- Harkness, J.S., Ruhl, L.S., Millot, R., Kloppman, W., Hower, J.C., Hsu-Kim, H., Vengosh, A., 2015. Lithium isotope fingerprints in coal and coal combustion residuals from the United States. In: Procedia Earth and Planetary Science, 11th Applied Isotope Geochemistery Conference AIG-11, pp. 134–137. https://doi.org/10.1016/j.proeps. 2015.07.032.
- Hauri, E.H., Shaw, A.M., Wang, J., Dixon, J.E., King, P.L., Mandeville, C., 2006. Matrix effects in hydrogen isotope analysis of silicate glasses by SIMS. Chem. Geol. 235, 352–365. https://doi.org/10.1016/j.chemgeo.2006.08.010.
- He, M.-Y., Luo, C., Lu, H., Jin, Z. dong, Deng, L., 2019. Measurements of lithium isotopic compositions in coal using MC-ICP-MS. J. Anal. At. Spectrom. 34, 1773–1778. https://doi.org/10.1039/C9JA00204A.
- Hervig, R.L., 1996. Analyses of geological materials for boron by secondary ion mass spectrometry. In: Grew, E.S., Anovitz, L.M. (Eds.), Boron Mineralogy, Petrology and Geochemistry, Reviews in Mineralogy. 33. Min Soc Am, Washington, DC, pp. 789–800.
- Hingston, F.J., 1964. Reactions between boron and clays. Austr J Soil Res 2, 83–95. https://doi.org/10.1071/sr9640083.
- Hong, H.-J., Ryu, T., Park, I.-S., Kim, M., Shin, J., Kim, B.-G., Chung, K.-S., 2018. Highly porous and surface-expanded spinel hydrogen manganese oxide (HMO)/Al₂O₃ composite for effective lithium (Li) recovery from seawater. Chem. Eng. J. 337, 455–461. https://doi.org/10.1016/j.cej.2017.12.130.
- Horstman, E.L., 1957. The distribution of lithium, rubidium and caesium in igneous and sedimentary rocks. Geochim. Cosmochim. Acta 12, 1–28. https://doi.org/10.1016/ 0016-7037(57)90014-5.
- Hosterman, J., 1990. Chemistry and mineralogy of natural bitumens and heavy oils and their reservoir rocks from the United States, Canada, Trinidad and Tobago, and Venezuela. U.S. Geol. Surv. Circ. 1047, 19. https://pubs.usgs.gov/circ/1990/1047/ report.pdf.
- Hunt, J.M., 1996. Petroleum Geochemistry and Geology. W.H. Freeman and Company, New York.
- Ishida, A., Kitajima, K., Williford, K.H., Tuite, M.L., Kakegawa, T., Valley, J.W., 2018. Simultaneous in situ analysis of carbon and nitrogen Isotope ratios in organic matter by secondary ion mass spectrometry. Geostand. Geoanal. Res. 42, 189–203. https://doi.org/10.1111/ggr.12209.
- Jin, H., 2014. Source Rock Potential of the Bakken Shales in the Williston Basin, North Dakota and Montana (Ph.D.). Colorado School of Mines, United States – Colorado.
- Jin, H., Sonnenberg, S.A., 2012. Source Rock Potential of the Bakken Shales in the Williston Basin, North Dakota and Montana. AAPG Search and Discovery Article #20156.
- Jones, R.W., 1981. Some mass balance and geological constraints on migration mechanisms. Am. Assoc. Pet. Geol. Bull. 65, 20. https://doi.org/10.1306/2F91977E-16CE-11D7-8645000102C1865D.
- Kavanagh, L., Keohane, J., Cabellos, G., Lloyd, A., Cleary, J., 2018. Induced plant accumulation of lithium. Geosci. J. 8, 56. https://doi.org/10.3390/geosciences8020056.
- Kesler, S.E., Gruber, P.W., Medina, P.A., Keoleian, G.A., Everson, M.P., Wallington, T.J., 2012. Global lithium resources: Relative importance of pegmatite, brine and other deposits. Ore Geol. Rev. 48, 55–69. https://doi.org/10.1016/j.oregeorev.2012.05.
- Ketris, M.P., Yudovich, Ya.E., 2009. Estimations of Clarkes for carbonaceous biolithes: world averages for trace element contents in black shales and coals. Int. J. Coal Geol. 78, 135–148. https://doi.org/10.1016/j.coal.2009.01.002.
- Lemarchand, E., Chabaux, F., Vigier, N., Millot, R., Pierret, M.-C., 2010. Lithium isotope

- systematics in a forested granitic catchment (Strengbach, Vosges Mountains, France). Geochim. Cosmochim. Acta 74, 4612–4628. https://doi.org/10.1016/j.gca.2010.04. 057.
- Lewan, M.D., Ruble, T.E., 2002. Comparison of petroleum generation kinetics by isothermal hydrous and nonisothermal open-system pyrolysis. Org. Geochem. 33, 1457–1475. https://doi.org/10.1016/S0146-6380(02)00182-1.
- Lewan, M.D., Comer, J.B., Hamilton Smith, T., Hasenmueller, N.R., Guthrie, J.M., Hatch, J.R., Gautier, D.L., Franki, W.T., 1995. Feasibility Study of Material-Balance Assessment of Petroleum from the New Albany Shale in the Illinois Basin. U.S. Geol. Surv. Bull. 2137, 40. https://pubs.usgs.gov/bul/2137/report.pdf.
- Littke, R., Leythaeuser, D., 1993. Migration of Oil and Gas in Coals: chapter 10. In: Rice, D.D. (Ed.), Law, B.E. Hydrocarbons from Coal, American Association of Petroleum Geologists, pp. 219–236.
- Liu, C., Wang, P., 2013. The role of algal blooms in the formation of lacustrine petroleum source rocks — evidence from Jiyang depression, Bohai Gulf Rift Basin, eastern China. Palaeogeogr. Palaeoclimatol. Palaeoecol. 388, 15–22. https://doi.org/10. 1016/j.palaeo.2013.07.024.
- Loftus, G.W.F., Greensmith, J.T., 1988. The lacustrine Burdiehouse Limestone Formation—a key to the deposition of the Dinantian Oil Shales of Scotland. Geol. Soc. Lond., Spec. Publ. 40, 219–234. https://doi.org/10.1144/GSL.SP.1988.040.01.19.
- Macpherson, G.L., 2015. Lithium in fluids from Paleozoic-aged reservoirs, Appalachian Plateau region, USA. Appl. Geochem. 60, 72–77. https://doi.org/10.1016/j. apgeochem.2015.04.013.
- Macpherson, G.L., Capo, R.C., Stewart, B.W., Phan, T.T., Schroeder, K., Hammack, R.W., 2014. Temperature-dependent Li isotope ratios in Appalachian Plateau and Gulf Coast Sedimentary Basin saline water. Geofluids 14, 419–429. https://doi.org/10.1111/cfl.12084.
- Matthews, J.P., Pisupati, S., 2018. Penn State and Argonne Premium Coal Sample Bank and Database. http://www.energy.psu.edu/cst/index.html.
- McCarthy, Kevin, Niemann, Martin, Palmowski, Daniel, Peters, Kenneth, Stankiewicz, Artur, et al., 2011. Basic petroleum geochemistry for source rock evaluation. Schlumberger oilfield review 23 (2), 32–43. In this issue. https://www.slb.com/-/media/files/oilfield-review/basic-petroleum.
- Meija, J., Coplen, T.B., Berglund, M., Brand, W.A., Bièvre, P.D., Gröning, M., Holden, N.E., Irrgeher, J., Loss, R.D., Walczyk, T., Prohaska, T., 2016. Atomic weights of the elements 2013 (IUPAC Technical Report). Pure Appl. Chem. 88, 265–291. https://doi.org/10.1515/pac-2015-0305.
- Millot, R., Vigier, N., Gaillardet, J., 2010. Behaviour of lithium and its isotopes during weathering in the Mackenzie Basin, Canada. Geochim. Cosmochim. Acta 74, 3897–3912. https://doi.org/10.1016/j.gca.2010.04.025.
- Millot, R., Guerrot, C., Innocent, C., Négrel, Ph., Sanjuan, B., 2011. Chemical, multiisotopic (Li-B-Sr-U-H-O) and thermal characterization of Triassic formation waters from the Paris Basin. Chem. Geol. 283, 226–241. https://doi.org/10.1016/j. chemsep.2011.01.020.
- Misra, S., Froelich, P.N., 2012. Lithium isotope history of Cenozoic seawater: changes in silicate weathering and reverse weathering. Science 335, 818–823. https://doi.org/ 10.1126/science.1214697.
- Mukhopadhyay, P.K., 1994. Vitrinite reflectance as maturity parameter: petrographic and molecular characterization and its applications to basin modeling. In: Mukhopadhyay, Prasanta K., Dow, W.G. (Eds.), Vitrinite Reflectance as a Maturity Parameter. American Chemical Society, Washington, DC, pp. 1–24. https://doi.org/ 10.1021/bk-1994-0570.ch001.
- Négrel, P., Millot, R., Brenot, A., Bertin, C., 2010. Lithium isotopes as tracers of groundwatercirculation in a peat land. Chem. Geol. 276, 119–127. https://doi.org/ 10.1016/j.chemgeo.2010.06.008.
- Nichols, D.J., Traverse, A., 1971. Palynology, petrology, and depositional environments of some early tertiary lignites in Texas. Proceedings of the Annual Meeting. American Association of Stratigraphic Palynologists 2, 37–48. https://doi.org/10.2307/ 3687276
- Nuccio, Vito, Hatch, Joseph, 1996. Vitrinite reflectance suppression in the New Alabany shale, Illinois Basin–vitrinite reflectance and rock-eval data. USGS Open file report, 96-665. https://pubs.usgs.gov/of/1996/0665/report.pdf.
- Orem, W.H., Finkelman, R.B., 2003. Coal formation and geochemistry. In: Holland, H.D., Turekian, K.K. (Eds.), Treatise on Geochemistry. Pergamon, Oxford, pp. 191–222. https://doi.org/10.1016/B0-08-043751-6/07097-3.
- Palmer, C.A., 1997. The chemical analysis of argonne premium coal samples. U.S. Geol. Surv. Bull. 2144, 106. https://pubs.usgs.gov/bul/b2144/b2144.pdf.
- Pawlewicz, M., Finn, T., 2002. Vitrinite reflectance data for the Greater Green River Basin, southwestern Wyoming, northwestern Colorado, and northeastern Utah. U.S. Geol Surv Open File Report 16, 02–339. https://pubs.usgs.gov/of/2002/ofr-02-0339/ofr-02-0339.pdf.
- Pendias, H., Kabata-Pendias, A., 2000. Trace Elements in Soils and Plants, Third edition. CRC Presshttps://doi.org/10.1201/9781420039900.
- Penniston-Dorland, S., Liu, X.-M., Rudnick, R.L., 2017. Lithium isotope geochemistry. Rev. Mineral. Geochem. 82, 165–217. https://doi.org/10.2138/rmg.2017.82.6.
- Peters, K.E., Cassa, M., 2007. Applied Source Rock Geochemistry. In: Magoon, L.B., Dow, W.G. (Eds.), The Petroleum System From Source to Trap. AAPG Memoir American Association of Petroleum Geologists, pp. 93–120. https://doi.org/10.1306/
- Peters, K.E., Xia, X., Pomerantz, A.E., Mullins, O.C., 2016. Chapter 3 geochemistry applied to evaluation of unconventional resources. In: Ma, Y.Z., Holditch, S.A. (Eds.), Unconventional Oil and Gas Resources Handbook. Gulf Professional Publishing, Boston, pp. 71–126. https://doi.org/10.1016/B978-0-12-802238-2.00003-1.

Petersen, H.I., 2006. The petroleum generation potential and effective oil window of humic coals related to coal composition and age. Int. J. Coal Geol. 67, 221–248. https://doi.org/10.1016/j.coal.2006.01.005.

- Phan, T.T., Capo, R.C., Stewart, B.W., Macpherson, G.L., Rowan, E.L., Hammack, R.W., 2016. Factors controlling Li concentration and isotopic composition in formation waters and host rocks of Marcellus Shale, Appalachian Basin. Chem. Geol. 420, 162–179. https://doi.org/10.1016/j.chemgeo.2015.11.003.
- Pistiner, J.S., Henderson, G.M., 2003. Lithium-isotope fractionation during continental weathering processes. Earth Planet. Sci. Lett. 214, 327–339. https://doi.org/10. 1016/S0012-821X(03)00348-0.
- Pittion, J.L., Gouadain, J., 1985. Maturity studies of the Jurassic 'Coal Unit' in three wells from the Haltenbanken area. In: Thomas, B.M. (Ed.), Petroleum Geochemistry in Exploration of the Norwegian Shelf. Springer, Netherlands, Dordrecht, pp. 205–211. https://doi.org/10.1007/978-94-009-4199-1 17.
- Qin, S., Zhao, C., Li, Y., Zhang, Y., 2015. Review of coal as a promising source of lithium. Int J Oil Gas Coal Tech 9, 215. https://doi.org/10.1504/IJOGCT.2015.067490.
- Saxby, J.D., 1976. Chapter 6 chemical separation and characterization of kerogen from oil shale. In: Yen, T.F., Chilingarian, G.V. (Eds.), Developments in Petroleum Science, Oil Shale. Elsevier, pp. 103–128. https://doi.org/10.1016/S0376-7361(08)70046-3.
- Seah, M.P., Shard, A.G., 2018. The matrix effect in secondary ion mass spectrometry. Appl. Surf. Sci. 439, 605–611. https://doi.org/10.1016/j.apsusc.2018.01.065.
- Sposito, G., Skipper, N.T., Sutton, R., Park, S., Soper, A.K., Greathouse, J.A., 1999. Surface geochemistry of the clay minerals. Proc. Natl. Acad. Sci. U. S. A. 96, 3358–3364. https://doi.org/10.1073/pnas.96.7.3358.
- Sun, Y., Zhao, C., Li, Y., Wang, J., Liu, S., 2012. Li distribution and mode of occurrences in Li-bearing coal seam# 6 from the Guanbanwusu Mine, Inner Mongolia, Northern China. Energy Explor. Exploit. 30, 109–130.
- Sun, H., Xiao, Y., Gao, Y., Zhang, G., Casey, J.F., Shen, Y., 2018. Rapid enhancement of chemical weathering recorded by extremely light seawater lithium isotopes at the Permian–Triassic boundary. Proc. Natl. Acad. Sci. U. S. A. 115, 3782–3787. https:// doi.org/10.1073/pnas.1711862115.
- Swaine, D.J., 1990. Mode of occurrence of trace elements in coal. In: Trace Elements in Coal. Elsevier, pp. 27–49. https://doi.org/10.1016/B978-0-408-03309-1.50008-3.
- Swanson, V., 1975. Collection, chemical analysis, and evaluation of coal samples in 1975.
 U.S. Geol Surv Open File Report 76-468, 503. https://doi.org/10.3133/ofr76468.
- Taylor, G.H., Teichmüller, M., Davis, A., Diessel, C.F.K., Littke, R., Robert, P., 1998.
 Organic Petrology, 1st ed. Gebrüder Borntraeger Verlagsbuchhandlung, Berlin, Germany.
- Tissot, B.P., Welte, D.H., 1984. Petroleum Formation and Occurrence. Springer-Verlag, New York (699 pp).
- Tissot, B.P., Pelet, R., Ungerer, P., 1987. Thermal history of sedimentary basins, maturation indices, and kinetics of oil and gas generation. AAPG Bull. 71, 1445–1466. https://doi.org/10.1306/703C80E7-1707-11D7-8645000102C1865D.
- Tomascak, P.B., Magna, T., Dohmen, R., 2016. Advances in Lithium Isotope Geochemistry, Advances in Isotope Geochemistry. Springer International Publishing, Cham. https://doi.org/10.1007/978-3-319-01430-2.
- Tonarini, S., Pennisi, M., Leeman, W.P., 1997. Precise boron isotopic analysis of complex silicate (rock) samples using alkali carbonate fusion and ion-exchange separation. Chem. Geol. 142, 129–137. https://doi.org/10.1016/S0009-2541(97)00087-9.
- Van Krevelen, D.W., 1950. Graphical-statistical method for the study of structure and reaction processes of coal. Fuel 29, 269–284.
- Vandenbroucke, M., Largeau, C., 2007. Kerogen origin, evolution and structure. Org. Geochem. 38, 719–833. https://doi.org/10.1016/j.orggeochem.2007.01.001.
- Vigier, N., Decarreau, A., Millot, R., Carignan, J., Petit, S., France-Lanord, C., 2008. Quantifying Li isotope fractionation during smectite formation and implications for the Li cycle. Geochim. Cosmochim. Acta 72, 780–792. https://doi.org/10.1016/j.gca. 2007.11.011.
- Vorres, K.S., 1990. The Argonne Premium Coal Sample Program. Energy Fuel 4, 420–426. https://doi.org/10.1021/ef00023a001.
- Williams, L.B., Bose, M., 2018. Measurements of the lithium isotope heterogeneity in coals and kerogen indicate an unrecognized lithium contribution to the global geochemical cycles. In: CMS 55th Annual Conference, Abstract, Urbana, IL., June 2018.
- Williams, L.B., Hervig, R.L., 2004. Boron isotope composition of coals: a potential tracer of organic contaminated fluids. Appl. Geochem. 19, 1625–1636. https://doi.org/10. 1016/j.apgeochem.2004.02.007.
- Williams, L.B., Hervig, R.L., 2005. Lithium and boron isotopes in illite-smectite: the importance of crystal size. Geochim. Cosmochim. Acta 69, 5705–5716. https://doi.org/10.1016/j.gca.2005.08.005.
- Williams, L.B., Clauer, N.C., Hervig, R.L., 2012. Light stable isotope microanalysis of clays in sedimentary rocks. In: Sylvester, Paul (Ed.), Quantitative Mineralogy and Microanalysis of Sediments and Sedimentary Rocks. Mineralogical Association of Canada Short Course 42. pp. 55–73.
- Williams, L.B., Środoń, J., Huff, W.D., Clauer, N., Hervig, R.L., 2013. Light element distributions (N, B, Li) in Baltic Basin bentonites record organic sources. Geochim. Cosmochim. Acta 120, 582–599. https://doi.org/10.1016/j.gca.2013.07.004.
- Williams, L.B., Crawford Elliott, W., Hervig, R.L., 2015. Tracing hydrocarbons in gas shale using lithium and boron isotopes: Denver Basin USA, Wattenberg Gas Field. Chem. Geol. 417, 404–413. https://doi.org/10.1016/j.chemgeo.2015.10.027.
- Wunder, B., Meixner, A., Romer, R.L., Feenstra, A., Schettler, G., Heinrich, W., 2007. Lithium isotope fractionation between Li-bearing staurolite, Li-mica and aqueous fluids: an experimental study. Chem. Geol. 238, 277–290. https://doi.org/10.1016/j. chemgeo.2006.12.001.